

Water Confined in Reverse Micelles: Acoustic and Densimetric Studies

A. Amararene,[†] M. Gindre, J.-Y. Le Huérou,* C. Nicot, W. Urbach,[‡] and M. Waks

Laboratoire d'Imagerie Paramétrique, URA CNRS 1458, 15 rue de l'École de Médecine,
F-75006 Paris, France, and Université René Descartes, 45 rue des Saints Pères, F-75005 Paris, France

Received: August 20, 1997[⊗]

We have used a custom-built ultrasound velocimeter to carry out high-precision velocity measurements of reverse micelle solutions, made of ionic (AOT) and nonionic (C₁₂E₄) surfactants in oil, as a function of water concentration. We show that the observed velocity variation as a function of increasing water concentration differs from the characteristics of the surfactant polar headgroups. The complex profile of compressibility curves obtained from velocity and densimetric measurements can be accounted for by the relation existing between the surface polar headgroup of each surfactant and the number of interacting water molecules. At the highest water concentration, the compressibility parameters obtained are different from those reported for “bulk” water and reflect the peculiar properties of confined water.

I. Introduction

Ultrasound velocity measurements carried out in solutions allow the determination of the compressibility of a fluid in relation to inter- and intramolecular interactions which can be characterized by the variation of thermodynamic parameters such as temperature, pressure, and volume. Solute–solvent and solute–solute interactions can also be investigated from values of the apparent compressibility. The solute–solute interaction contribution to the apparent compressibility decreases with solute concentration and thus the apparent compressibility reflects at low concentration the contribution of the solute intrinsic compressibility and solute–solvent interactions. These considerations also hold for complex fluids which exhibit a characteristic length of scale larger than that of the molecular assemblies constituting the fluid.¹

In this regard, water-in-oil reverse micelles² seem particularly relevant. They are water microdroplets of variable size, dispersed in nonmiscible apolar solvents and stabilized by a monolayer of surfactant. The size of these droplets, which are thermal equilibrium structures, depends only on water concentration defined as the water-to-surfactant molar ratio W_0 . When water is added to the surfactant solution, the micelles swell, and their radius increases independently of the concentration of droplets while their total number drops.

There exists to date a wealth of knowledge about the unusual physical–chemical properties of encapsulated water in reverse micelles in particular that of the anionic surfactant sodium bis-(2-ethylhexyl) sulfosuccinate (AOT) in oil, obtained by a number of physical techniques.^{3–5} In general, water properties in nonionic surfactants are much less documented.

We present in this report a study of sound propagation in two different complex fluid systems made of water, oil, and ionic and nonionic surfactants, as a function of water concentration. We have used high-precision sound velocity and density experiments to characterize further water–surfactant interactions at micellar interfaces and to obtain additional insights on the properties of sequestered water. To the best of our knowledge, there are no other reports providing values for the adiabatic

compressibility of water encapsulated in such organized assemblies, as a function of water concentration. Ultrasonic measurements of small liquid volumes require a high-precision instrumentation such as the experimental setup, based on frequency measurements, described previously by Sarvazyan.⁶ In our laboratory, we have developed a different ultrasound precision velocimeter and we have carried out velocity measurements of water sequestered in the micellar core. We show a close relation between the adiabatic compressibility of encapsulated water and the chemical nature of the surfactant used in reverse micelles. In all experiments, the measured values are different from that reported for “bulk” water. The difference can be accounted for by the various forces generated between the surface polar headgroups and water molecules confined in limited space.

II. Theoretical Background

A. Adiabatic Compressibility. To evaluate the elastic properties of an homogeneous isotropic medium such as for example an aqueous solution, we use β , the adiabatic compressibility:⁷

$$\beta = -\frac{1}{V} \left(\frac{\partial V}{\partial P} \right) \quad (1)$$

where $(\partial V/\partial P)$ is the volume variation with applied pressure at constant entropy and V the volume of the solution.

The adiabatic compressibility β is related to the sound velocity u and to the density ρ by the well-known Laplace equation:

$$\beta = 1/\rho u^2 \quad (2)$$

B. Apparent Specific Volume. The apparent specific volume φ_V or inverse of the density, ρ_s^{-1} , of the solute can be determined from solution and solvent densities, as follows:

$$\varphi_V = \frac{1}{\rho_s} = \frac{V_s}{V} \frac{V}{m_s} = \frac{V_s}{V} \frac{1}{C}$$

where V is the volume of the solution, V_s and m_s are respectively the volume and the mass of the solute, and C is its concentration. Thus, according to⁸

* Corresponding author.

[†] Université René Descartes.

[‡] Laboratoire de Physique Statistique de l'École Normale Supérieure URA CNRS 1306, 24 rue Lhomond, F-75005 Paris, France.

[⊗] Abstract published in *Advance ACS Abstracts*, November 15, 1997.

$$\varphi_V = \frac{V - V_0}{VC} \quad (3)$$

where V_0 is the volume of the solvent. By expressing volumes as a function of masses and densities

$$\varphi_V = \frac{\frac{m}{\rho} - \frac{m - m_s}{\rho_0}}{VC} \quad (4)$$

where ρ_0 is the density of the solvent and ρ is the density of the solution, respectively. Developing eq 4, one can express φ_V as a function of densities ρ_0 and ρ and of concentration C :

$$\varphi_V = \frac{1}{\rho_0} - \frac{\rho - \rho_0}{\rho_0 C} \quad (5)$$

C. Effective Medium Theory. In this report we use the effective-medium theory⁹ to account for the behavior of a multicomponent system constituted of reverse micelles in organic solvents. Each of the constituent phases of the system is described by parameters pertaining to the pure phase. The theory can evaluate the adiabatic compressibility of the complex medium as a function of the relative volumes of constituent phases. It can be applied to the present work, since the acoustic wavelength (100×10^{-6} m) is several orders of magnitude larger than the size of reverse micelles (radius in the $(15-50) \times 10^{-10}$ m range). The measured compressibility (β) value of the solution is then composed of several terms:

$$\beta = \beta_s \Phi_s + \beta_0 \Phi_0 \quad (6)$$

where $\Phi_s = V_s/V = (V - V_0)/V$ is the volume fraction of the solute, $\Phi_0 = V_0/V$ is the volume fraction of the solvent, and β_s and β_0 are adiabatic compressibilities of the solute and the solvent, respectively. Note that the volume fractions are also related to the apparent specific volume φ_V and to the concentration C of the solute: as $\Phi_s = C\varphi_V$ and $\Phi_0 = 1 - C\varphi_V$. Equation 6 can be written as

$$\beta_s = \frac{\beta - \beta_0(1 - C\varphi_V)}{C\varphi_V} \quad (7)$$

In this work we have determined φ_K , the apparent specific adiabatic compressibility of a solute, defined by the expression

$$\varphi_K = \frac{\beta V - \beta_0 V_0}{CV} \quad (8)$$

Rearranging eq 3 with eq 8 leads to

$$\varphi_K = \beta_0 \left(\frac{\beta - \beta_0}{\beta_0 C} + \varphi_V \right); \quad \varphi_K = \frac{\beta - \beta_0(1 - C\varphi_V)}{C} \quad (9)$$

When comparing eqs 9 and 7, φ_K can be related to β_s , calculated by the effective medium theory

$$\varphi_K = \beta_s \varphi_V \quad (10)$$

In this work we denote density and sound velocity specific relative concentrational increments by square brackets $[\rho]$ and $[u]$, as suggested by Sarvazyan.¹⁰ Thus, differentiating eq 2, and dividing by C one obtains

$$\frac{\beta - \beta_0}{\beta_0 C} = -2 \frac{u - u_0}{u_0 C} - \frac{\rho - \rho_0}{\rho_0 C} = -2[u] - [\rho] \quad (11)$$

Replacing this value in eqs 9 and 5 leads to

$$\varphi_K = \beta_0 \left(2\varphi_V - 2[u] - \frac{1}{\rho_0} \right) \quad (12)$$

where β_0 and ρ_0 are constant parameters, independent of concentration C . Thus the variations of φ_K observed depend solely on the experimental determination of $[u]$ the relative specific increment of sound velocity and on φ_V , the apparent specific volume. Note that eq 12 is only valid at low solute concentration.

III. Experimental Section

A. Materials. AOT was purchased from Sigma (SigmaUltra) 99% pure and used after desiccation in vacuum over phosphorus pentoxide (Sicapent from Merck). The nonionic surfactant, tetraethylene glycol monododecyl ether ($C_{12}E_4$), was obtained from Nikko Chemicals and judged to be >99% pure from gas chromatography. Isooctane, Pro Analyti grade, was from Merck and decane, >99% pure, from Sigma. Water used in this study was of MilliQ purity.

B. Sample Preparation. All the samples were prepared by weighing the solutes (surfactant and water) on a Model 1712 Sartorius balance, in precision volumetric flasks (class A ± 0.04 mL), with a precision of ± 0.03 mg. The solvents used to make up the volume at 20 °C were either pure organic solvents or organic solutions of the surfactant, which were prepared and used as a mixed solvent.¹¹ The maximum error introduced by this procedure does not exceed the reported error limits.

C. Volumetric Measurements. The densities $\rho(C)$ of solutions, at increasing solute concentrations C , were determined at 25.00 ± 0.01 °C using the vibrating tube Anton Paar DMA 58 digital density meter. The precision obtained is of the order of $\pm 5 \times 10^{-3}$ kg m⁻³. Each determination was carried out at least five times and averaged. The value was used to calculate the apparent specific volume.

D. Ultrasound Velocity Measurements. Several methods of ultrasound velocity determination have been described to date: time of flight measurements,¹² the sing-around method,¹³ resonance methods,¹⁴ and the phase comparison method.¹⁵ Among them we have selected the method based on time of flight determination which offers, in addition to its simplicity, a high precision permitted by recent instrumental advances.

1. Principle. In ultrasound velocity measurements using the time of flight, a short electrical pulse is applied to a piezoelectrical transducer, converting the electrical wave into an acoustical one, propagating through the studied medium. A second transducer converts in turn the received wave into an electrical signal, which is compared to the excitation signal. The time interval elapsed between the two signals allows the determination of the ultrasound velocity, knowing the precise distance between the two transducers.¹⁶

2. Measurement System. Although the method seems simple *per se*, one of the principal limitations of the system resides in possible temperature drifts. This difficulty is circumvented by the use of a set of tandem cells of identical acoustic path,⁶ enclosed in a single metal block. It allows the sequential determination of the ultrasonic velocity difference between a reference and a measuring cell at identical temperature conditions and thus achieves a considerable improvement in sensitivity. First, the two cell acoustic paths are filled with the reference liquid and the velocity measurements are carried out. In a second step, the measuring cell is drained, rinsed, dried, and refilled with the liquid under investigation.

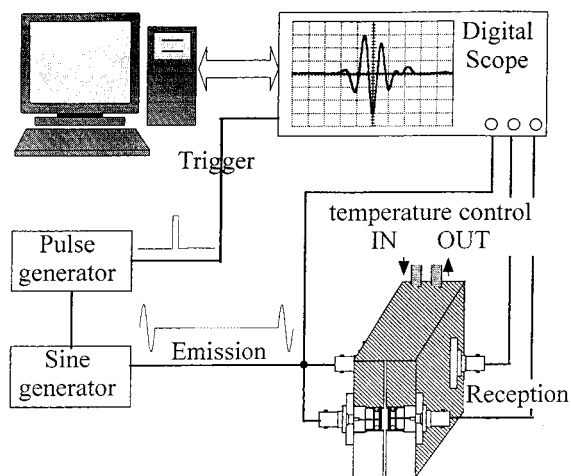


Figure 1. Scheme of the ultrasound velocity experimental setup. For details see text.

The experimental setup is illustrated on Figure 1. Briefly it is composed of the two tandem cells (volume 3 mL), a signal generator delivering a 10 MHz sine signal, and a pulse generator allowing the modulation of the sine signal amplitude to obtain the excitation signal of the emitting transducers. In order to always start at a zero voltage level, the pulse duration is adjusted to be a multiple of the sine period. A digital oscilloscope (Lecroy Model 9424E), synchronized with the pulse generator, samples the excitation signal as well as signals issued by the two transducers—receivers. Measurements have been automated by a PC computer equipped with an IEEE interface, which processes all the data. All the parameters characterizing the excitation signal, i.e., amplitude of the excitation signal, duration of the pulse, pulse period, and emission frequency of the ultrasound wave, have been optimized for maximal precision.

3. Procedures and Experimental Performances. The thermal stability of the experimental setup is maintained at 25 °C by a Huber SH 40 circulating thermostat. As mentioned above, the internal temperature stability is checked by the periodic monitoring of ultrasound velocity in the reference cell. Under our experimental conditions, the temperature stability is in the order of 10^{-4} ; nevertheless, the observed temperature drift is less than 10^{-5} per 24 h. Velocity determinations are carried out every 2 min for periods of 20 min. For each concentration of the solute, the ultrasound velocity is measured within each cell and the difference calculated. For every run, the signal is averaged over 100 acquisitions in order to increase the signal-to-noise ratio. The time-to-velocity conversion requires a precise determination of the distance between the two transducers. For this purpose a calibration is carried out with a solvent in which the ultrasound velocity is known with an accuracy better than 10^{-5} . (The latter sound velocity value should be close to the velocity in the sample.) For example, pure methanol and ethanol have been used and the distance was calculated from the measured time of flight.

For a better precision of the time of flight, the temporal position of the energetic gravity center (barycenter method) of the captured signal is searched. The signal is analyzed in a

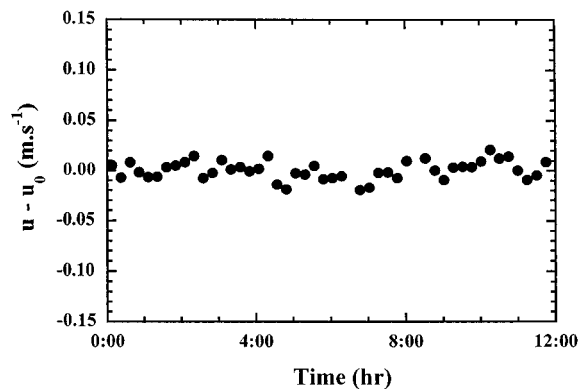


Figure 2. Plot of the absolute deviation in velocity $u - u_0$ vs time. The experiment was carried out with distilled water at 25 °C.

window composed of N samples, separated by a time interval Δt , starting at time t_d . The equation used for the barycenter (t_p) calculation is classical:

$$t_p = t_d + \frac{\sum_{i=0}^{N-1} i \Delta t A_i^2}{\sum_{i=0}^{N-1} A_i^2} \quad (13)$$

where A_i is the amplitude of the i th sample. The time spacing between two consecutive samplings (Δt) is 0.1 ns.

The shift in the velocity occurring between the two cells over a period of 12 h is represented on Figure 2. It clearly appears that the absolute deviation observed in velocity, (designated as $u - u_0$) is in the order of $0.02 \text{ m}\cdot\text{s}^{-1}$, the standard deviation being smaller than $1 \text{ cm}\cdot\text{s}^{-1}$. The final precision in ultrasound velocity determination is better than 10^{-5} .

IV. Results

In the first set of experiments, we have determined the volumetric and the compressibility parameters of the two surfactants used (AOT and C_{12}E_4) in their respective solvents, isooctane and decane. In addition, we have characterized by the same procedure AOT in decane. The variation of φ_K and φ_V plotted as a function of surfactant concentration (not shown) indicates in all cases a linear dependence for surfactant concentrations above the critical micelle concentration (cmc), the surfactant concentration above which micelles form. At low concentration, ultrasound velocity curves of C_{12}E_4 in decane display a clear breaking point corresponding to the cmc.

The extrapolation of φ_K and φ_V , when C tends to zero, yields values of $\lim_{C \rightarrow 0} \varphi_V = 0.879 \times 10^{-3} \text{ m}^3 \cdot \text{kg}^{-1}$ for AOT in isooctane and $1.073 \times 10^{-3} \text{ m}^3 \cdot \text{kg}^{-1}$ for C_{12}E_4 in decane, while the values of $\lim_{C \rightarrow 0} \varphi_K$ obtained for AOT and C_{12}E_4 are respectively 36.4 and $48.9 \times 10^{-14} \text{ Pa}^{-1} \cdot \text{m}^3 \cdot \text{kg}^{-1}$. For AOT in decane $\lim_{C \rightarrow 0} \varphi_V = 0.888 \times 10^{-3} \text{ m}^3 \cdot \text{kg}^{-1}$ and $\lim_{C \rightarrow 0} \varphi_K = 40.6 \times 10^{-14} \text{ Pa}^{-1} \cdot \text{m}^3 \cdot \text{kg}^{-1}$. Finally, from eq 10 we have calculated β_s . All the data are summarized on Table 1.

TABLE 1: Volumetric and Compressibility Data of AOT and C_{12}E_4 at 25 °C^a

	$\lim_{C \rightarrow 0} \varphi_V$ ($10^{-3} \text{ m}^3 \cdot \text{kg}^{-1}$)	$\lim_{C \rightarrow 0} [u]$ ($10^{-3} \text{ m}^3 \cdot \text{kg}^{-1}$)	$\lim_{C \rightarrow 0} \varphi_K$ ($10^{-14} \text{ Pa}^{-1} \cdot \text{m}^3 \cdot \text{kg}^{-1}$)	$\lim_{C \rightarrow 0} \beta_s$ (10^{-11} Pa^{-1})
AOT in decane	0.888 ± 0.001	-0.025 ± 0.001	40.6 ± 0.8	41.4 ± 0.8
AOT in isooctane	0.879 ± 0.001	0.006 ± 0.001	36.4 ± 0.4	45.7 ± 0.2
C_{12}E_4 in decane	1.073 ± 0.001	0.114 ± 0.002	48.9 ± 0.2	45.6 ± 0.2

^a The parameters have been extrapolated at concentration $C = 0$.

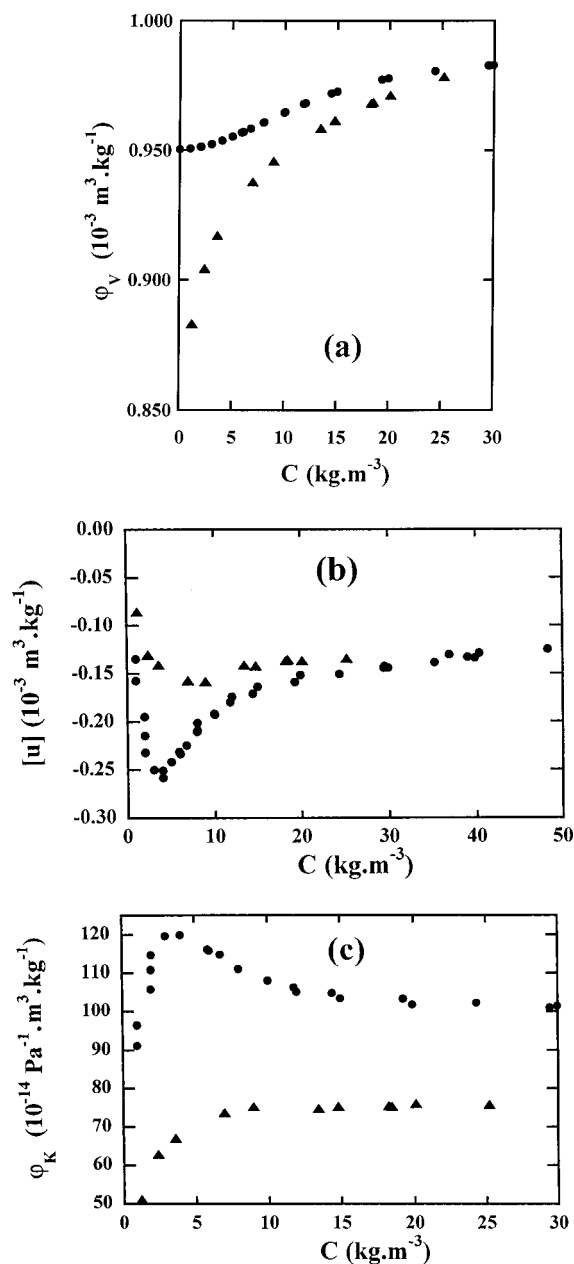


Figure 3. Plot of the volumetric and ultrasound velocity parameters as a function of water concentration C : ●, AOT reverse micelles; ▲, C_{12}E_4 reverse micelles. The concentration of AOT and C_{12}E_4 is 0.1 M and the temperature 25 °C. In all figures, the experimental points represent the average value of at least 3–5 measurements. (a) Variation of φ_v , the apparent specific volume of water. (b) Variation of $[u]$, the relative specific velocity increment. (c) Variation of φ_K , the apparent specific adiabatic compressibility.

In the next set of experiments, organic solutions of the surfactants at 0.1 M concentration were used as mixed solvents while water was taken as the solute. The variation of φ_v , the apparent specific volume, $[u]$, the relative specific velocity increment, and φ_K , the apparent specific adiabatic compressibility of the solubilized water, plotted as a function of water concentration, are illustrated in Figure 3, a, b, and c, for AOT reverse micelles in isooctane and for C_{12}E_4 reverse micelles in decane. In both cases, a variation of φ_K and φ_v is observed for increasing water concentration. The difference between the curve profiles obtained for each surfactant is striking.

A. AOT. The plot of φ_v vs C expressed on a weight basis in $\text{kg}\cdot\text{m}^{-3}$ (Figure 3a) shows that the overall relative variation of the volume, $\Delta\varphi_v/\varphi_v$ is of the order of 3.5%. A detailed analysis reveals that the curve can be divided into three

segments. The first one, starting at a φ_v value of $0.950 \times 10^{-3} \text{ m}^3\cdot\text{kg}^{-1}$, shows little variation and extends to a micellar water concentration of $4 \text{ kg}\cdot\text{m}^{-3}$; the second corresponds to the midcurve inflection point at a water concentration around $11 \text{ kg}\cdot\text{m}^{-3}$. The final part of the curve starting at $C = 25 \text{ kg}\cdot\text{m}^{-3}$ is almost a plateau.

The curve obtained from ultrasound velocity measurements is rather complex (Figure 3b), indicating that the $[u]$ value is very sensitive to small changes in water concentration. The initial part of the curve decreases steadily down to $-0.25 \times 10^{-3} \text{ m}^3\cdot\text{kg}^{-1}$, reaching its minimum value for a water concentration in the 3.0 – $4.0 \text{ kg}\cdot\text{m}^{-3}$ range. Then $[u]$ increases rapidly, attaining a value of $-0.17 \times 10^{-3} \text{ m}^3\cdot\text{kg}^{-1}$ for a water concentration of $15 \text{ kg}\cdot\text{m}^{-3}$. The final part of the curve, where $[u]$ seems to increase exponentially, illustrates a smooth return to the first value measured.

The curve illustrating the variation of φ_K vs C (Figure 3c) looks very much like a mirror image of curve b, indicating that in the ionic surfactant, the velocity (and not φ_v), represents indeed the predominant factor of the observed phenomenon. The maximum of compressibility ($120 \times 10^{-14} \text{ Pa}^{-1}\cdot\text{m}^3\cdot\text{kg}^{-1}$) is attained for a water concentration in the range of 3 – $4 \text{ kg}\cdot\text{m}^{-3}$, the plateau corresponding then to a value of $100 \times 10^{-14} \text{ Pa}^{-1}\cdot\text{m}^3\cdot\text{kg}^{-1}$.

B. C_{12}E_4 . If we turn now to the variation of φ_v , $[u]$, and φ_K with water concentration for C_{12}E_4 reverse micelles in decane, it is obvious that the picture emerging is quite different, as also illustrated in Figure 3a–c. The change of φ_v vs concentration shows a monotonic increase, the overall relative variation of φ_v being higher (10%) compared to that of AOT. The velocity increment $[u]$ drops rapidly as water concentration increases, reaching a smooth minimum around a value of $-0.16 \times 10^{-3} \text{ m}^3\cdot\text{kg}^{-1}$ and then grows steadily until a value of $-0.13 \times 10^{-3} \text{ m}^3\cdot\text{kg}^{-1}$. Finally, the compressibility parameter φ_K , starting at a lower initial value than in AOT ($50 \times 10^{-14} \text{ Pa}^{-1}\cdot\text{m}^3\cdot\text{kg}^{-1}$), increases rapidly reaching a plateau located around a value of $75 \times 10^{-14} \text{ Pa}^{-1}\cdot\text{m}^3\cdot\text{kg}^{-1}$, for a concentration of water at $8 \text{ kg}\cdot\text{m}^{-3}$. The plateau originates from the very slight increase of both φ_v and $[u]$.

V. Discussion

Surfactants in oil aggregate, due to a very low level of residual water (ref 2) (less than 0.5 water molecule per surfactant polar headgroup) and they form “dry micelles” above a critical micelle concentration.¹⁷ As shown in Table 1, although the compressibility of pure isooctane has a higher value than that of decane (121 and $90 \times 10^{-11} \text{ Pa}^{-1}$, respectively), both φ_v and β_s , which are directly related to volume and compressibility of “dry” AOT aggregates, have a smaller value in isooctane than in decane. This is probably due to the better penetration of the branched solvent (isooctane) around the branched tails of the surfactant AOT.¹⁸ Note that in decane, both surfactants display a very similar β_s value.

Now, we examine the results in terms of the number of water molecules interacting with one surfactant headgroup. For the ionic surfactant, the water-to-surfactant molar ratio (W_0) is defined as $[\text{H}_2\text{O}]/[\text{AOT}]$ since the cmc is negligible (2). For the nonionic surfactant this does not hold as a higher value of cmc has to be taken into account for W_0 determination. This constant was measured for C_{12}E_4 in decane, at 25 °C ($1.18 \text{ g}/100 \text{ mL}$) by a spectroscopic technique described elsewhere.¹⁹ It compares well with the value obtained from ultrasound velocity measurements ($1.05 \text{ g}/100 \text{ mL}$). The micellar water content of the solution is then expressed as

$$(W_0)_{\text{mic}} = \frac{[\text{H}_2\text{O}]}{[\text{C}_{12}\text{E}_4] - ([\text{C}_{12}\text{E}_4]_{\text{cmc}})} \quad (14)$$

Figure 4, a, b, and c, compare volumetric, velocity, and compressibility data, as a function of W_0 for both surfactants. We can now relate the data to the number of interacting water molecules per surfactant headgroup.

A. Volumetric Measurements. At first glance on Figure 4a, it is striking that the specific volume of micellar water molecules measured in both surfactants yields always values lower than that reported for "bulk" water ($1.003 \times 10^{-3} \text{ m}^3 \cdot \text{kg}^{-1}$). In AOT reverse micelles a detailed analysis reveals that the initial segment of the curve implies the binding of the first two or three water molecules. The midpoint of the volumetric curve corresponds to 6–7 interacting water molecules. The final segment of the curve, almost a plateau, begins at a W_0 value of 13 and extends to $W_0 = 27$. The measured φ_V values indicate a contracted volume for water, of the same order of magnitude as that observed in ion–water interactions of sodium chloride solutions,²⁰ but less than that calculated for biological membranes.²¹

Considering now the shape of the curve illustrating the variation of φ_V as a function of W_0 in C_{12}E_4 reverse micelles (Figure 4a), the progressive increase of water volume is consistent with the description of an early water segregation in the micellar core before the completion of surfactant hydration.²² The low φ_V values reported in this work reflect the presence of micellar water of high density. Under quite different experimental conditions, the structure of water in the nonionic surfactant has been previously explored by Raman scattering.²³ In concentrated aqueous solution of C_{10}E_5 (a parent surfactant molecule) the analysis of the OH stretching vibrations revealed a very large amount of bound water and a local environment around the surfactant headgroup displaying water molecules of density lower than "bulk" water. Note that hydration of the hydrophilic polar headgroup is a crucial factor determining the micellar surface curvature and hence the phases (normal or reverse).^{24,25} The existence of a high dense water in our ternary reverse system compared to the low dense water described in a binary aqueous system is then not surprising and constitutes an interesting finding.

B. Compressibility Measurements. Comparison of the shapes of the $[u]$ curves as a function of W_0 (Figure 4b) reveals a striking contrast in the behavior of the 13 first water molecules, interacting with the ionic and nonionic surfactants, whereas at high W_0 values the two curves look quite similar. Considering now the apparent compressibility curve of water in AOT reverse micelles, clear inflection points occur at W_0 values of 3 and 6 (Figure 4c).

Under conditions of extremely low water concentration, we are still dealing with almost "dry micelles" and, as noted by Ye et al.,¹ the solid core of the tightly packed headgroups of the AOT molecules is much more rigid than the suspending fluid. The first 2–3 water molecules hydrate the immediately adjacent anionic sulfonate (SO_3^-) groups and bind them very strongly, even at a low charge density.²⁶ Their action contributes thus to "lubricate" the dry surfactant molecular aggregates with a water of increased molecular mobility. These waters induce a stronger hydration of the anions, designated as kaotropes,²⁶ and bring about a large increase of the apparent specific compressibility (up to $120 \times 10^{-14} \text{ Pa}^{-1} \cdot \text{m}^3 \cdot \text{kg}^{-1}$). Upon the addition of the next three water molecules, reverse micelles start to self-organize and hydration proceeds to Na^+ counterions of the AOT polar headgroups, which act as a weak kosmotropes,²⁷ decreasing the mobility of nearby water molecules, and leading

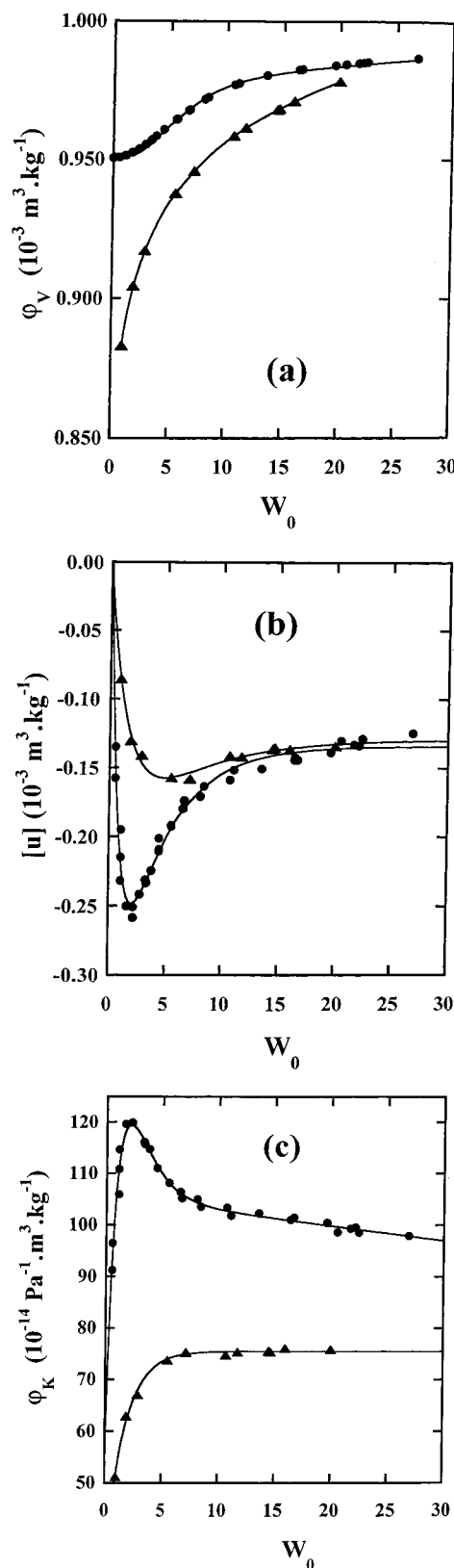


Figure 4. Plot of the volumetric and ultrasound velocity parameters as a function of W_0 the water to surfactant molar ratio: ●, AOT reverse micelles; ▲, C_{12}E_4 reverse micelles. (a) Variation of φ_V , the apparent specific volume of water. (b) Variation of $[u]$, the relative specific velocity increment. (c) Variation of φ_K , the apparent specific adiabatic compressibility. Same experimental conditions as in Figure 3. The continuous line is a guide for the eye.

to electrostricted water of higher density and lower compressibility.^{20,28,29} Taken together, these events lead obviously to the decrease of φ_K as shown in Figure 4c. With subsequent

addition of water, the micelles grow in size, reaching a plateau value, yet the final compressibility value remains always higher than that of "bulk" water, i.e. $\beta = 45 \times 10^{-11} \text{ Pa}^{-1}$.

The interaction of water molecules with AOT in reverse micelles has been previously investigated by Hauser et al.,⁴ using proton nuclear magnetic resonance spectroscopy, electron spin resonance, and difference scanning calorimetry. Their conclusion was that, although 2–4 water molecules are in the tightest interaction with a single AOT molecule, overall up to 13 water molecules remain severely perturbed. They also found that all but the last six water molecules freeze upon cooling AOT reverse micelles to -50°C . More recently, Christopher et al.⁵ carried out a Fourier transform infrared spectroscopic study of the water–headgroup interactions in AOT reverse micelles. These investigators reached very similar conclusions: namely, that the first three water molecules are strongly hydrogen-bonded to the anion. Addition of three water molecules per headgroup results in a solvated cation. Yet, according to these authors, the water environment of an AOT polar headgroup remains highly perturbed up to 13 water molecules ($W_0 = 13$), i.e., until the second solvation shell is completed. These results are in good agreement with the compressibility and densimetric data reported above.

Turning our attention to C_{12}E_4 compressibility curves (Figure 4c), we can also relate the initial value obtained for φ_K ($50 \times 10^{-14} \text{ Pa}^{-1} \cdot \text{m}^3 \cdot \text{kg}^{-1}$), to the tight packing of the "dry" surfactant polar headgroups. Then, the rapid increase of φ_K originates from the addition of the first water molecules, relaxing the surfactant aggregates by a "lubricating effect" involving four water molecules (i.e., one per oxyethylene group), similar to that observed in the water–AOT interaction. However, since the nonionic surfactant does not carry charged groups, we observe afterwards the presence of continuous plateau reflecting only the monotonous increase of micellar size. The final compressibility has also a higher value compared to that of "bulk water".

VI. Conclusions

From the present work, it is obvious that the differences measured for φ_V , $[u]$, and φ_K at low water content represent essentially the perturbation brought by water molecules interacting with polar headgroups of different chemical nature, charge, and polarity.³⁰ Such interactions obviously modify the complex hydrogen-bonding network existing in water, perturbing its specific volume and compressibility as reported above. Our results also agree with the findings of Bloor et al.,³¹ who observed a strong dependence of the micellar compressibility on the chemical nature of the surfactant polar headgroup, clearly illustrated in Figure 4c.

Under the experimental conditions described herein, it is notable that even at the highest water concentration measured, the apparent specific volume and adiabatic compressibility of water in reverse micelles never reach a value of "bulk" water. Such a result is in agreement with similar observations previously reported for other physical parameters of water measured in reverse micelles.² Thus it may be possible that the compress-

ibility values found in this work may be comparable to that existing in water-confined spaces.³²

The above results also suggest future directions of research concerning the acoustic and volumetric properties of water, in particular that existing in the various phases which occur in ternary systems of the nonionic surfactant family studied here, as well as that of water in immediate contact of proteins. As shown above, they can be precisely measured in self-assembled membrane–mimetic systems.

Acknowledgment. This research was supported in part by Centre National de la Recherche Scientifique (program ULTIMATECH) and by Institut National de la Santé et de la Recherche Médicale (CRE # 920920 to M.W.). The authors are grateful to Pr. B. Nongaillard for invaluable help. They thank Pr. A. Sarvazyan, Pr. T. Chalikian, and Pr. P.C. Kahn for many stimulating and fruitful discussions.

References and Notes

- (1) Ye, L.; Weitz, A.; Sheng, P.; Huang, J. S. *Phys. Rev. A* **1991**, *44*, 8249.
- (2) Luisi, P. L.; Magid, L. J. *CRC Crit. Rev. Biochem.* **1986**, *20*, 409.
- (3) Llor, A.; Zemb, T. *Structure and Reactivity in Reverse Micelles*; Pileni, M. P., Ed.; Elsevier: Amsterdam, 1989; p 54.
- (4) Hauser, H.; Haering, G.; Pande, A.; Luisi, P. L. *J. Phys. Chem.* **1989**, *93*, 7869.
- (5) Christopher, D. J.; Yarwood, J.; Belton, P. S.; Hills, B. P. *J. Colloid Interface Sci.* **1992**, *152*, 465.
- (6) Sarvazyan, A. P. *Ultrasonics* **1982**, *20*, 151.
- (7) Morse, P. M.; Ingard, K. U. *Theoretical Acoustics*; Princeton University Press: Princeton, NJ, 1986; p 280.
- (8) Zamyatin, A. A. *Annu. Rev. Biophys. Bioeng.* **1984**, *13*, 145.
- (9) Sheng, P. *Homogenization and Effective Moduli of Materials and Media*; Eriksen, J. L., Kinderleher, D., Kohn, R., Lions, J. L., Eds.; Springer-Verlag: New York, 1983; p 196.
- (10) Sarvazyan, A. P. *Annu. Rev. Biophys. Biophys. Chem.* **1991**, *20*, 321.
- (11) Wang, L.; Verall, R. E. *J. Colloid. Interface Sci.* **1993**, *160*, 380.
- (12) May, J. E. *Precise measurement of time delay*; IRE Natl. Conv. Rec. **6**, 1958, Pt2.
- (13) Cedrone, N. P.; Curran, D. R. *J. Acoust. Soc. Am.* **1954**, *26*, 963.
- (14) Fry, W. J. *J. Acoust. Soc. Am.* **1949**, *21*, 17.
- (15) Rogez, D.; Bader, M. *J. Acoust. Soc. Am.* **1984**, *76*, 167.
- (16) Del Grosso, V. A.; Mader, C. W. *J. Acoust. Soc. Am.* **1972**, *52*, 961.
- (17) O'Connor, C. J.; Lomax, T. D.; Ramage, R. E. *Adv. Colloid. Interface Sci.* **1984**, *20*, 21.
- (18) Fletcher, P. D. I.; Howe, A. M.; Robinson, B. H. *J. Chem. Soc., Faraday Trans. 1* **1987**, *83*, 985.
- (19) Merdas, A.; Gindre, M.; Ober, R.; Nicot, C.; Urbach, W.; Waks, M. *J. Phys. Chem.* **1996**, *100*, 15180.
- (20) Onori, G. *J. Chem. Phys.* **1988**, *89*, 510.
- (21) Scherer, J. R. *Proc. Natl. Acad. Sci. U.S.A.* **1987**, *84*, 7938.
- (22) Caldaru, H.; Caragheorghopol, A.; Vasilescu, M.; Dragutan, I.; Lemmetyinen, H. *J. Phys. Chem.* **1994**, *98*, 5320.
- (23) Micali, N.; Vasi, C.; Malmace, F.; Corti, M.; Degiorgio, V. *Phys. Rev. E* **1993**, *48*, 3661.
- (24) Corti, M.; Degiorgio, V. *Phys. Rev. Lett.* **1985**, *55*, 2005.
- (25) Lee, D. D.; Chen, S. H. *Phys. Rev. Lett.* **1994**, *73*, 106.
- (26) Collins, K. D. *Proc. Natl. Acad. Sci. U.S.A.* **1995**, *92*, 5553.
- (27) Collins, K. D. *Biophys. J.* **1997**, *72*, 65.
- (28) Onori, K. G.; Santucci, A. *J. Chem. Phys.* **1990**, *63*, 2939.
- (29) Marcus, Y. *J. Chem. Soc., Faraday Trans.* **1993**, *89*, 713.
- (30) Wang, L. R.; Verall, E. *J. Phys. Chem.* **1994**, *98*, 4368.
- (31) Bloor, D. M.; Gormally, J.; Jones, E. W. *J. Chem. Soc., Faraday Trans. 1* **1984**, *80*, 1915.
- (32) Minton, A. P. *Biophys. J.* **1995**, *68*, 1311.